HSV-1 strains circulating in Finland demonstrate uncoupling of geographic and phenotypic variation

[1]Christopher D. Bowen, [2#]Henrik Paavilainen, [1#]Daniel W. Renner, [2]Jussi Palomäki, [2]Jenni Lehtinen, [2]Tytti Vuorinen, [3]Peter Norberg, [2*]Veijo Hukkanen, [1*]Moriah L. Szpara

[1]Department of Biochemistry and Molecular Biology, Center for Infectious Disease Dynamics, and the Huck Institutes of the Life Sciences, Pennsylvania State University, University Park, Pennsylvania 16802, USA
[2]Department of Virology, University of Turku, Kiinamyllynkatu 13, FIN-20520 Turku, Finland
[3]Department of Virology, University of Gothenburg, Gothenburg, Sweden

#equal contribution of DWR and HP
***equal contribution of MLS and VH**

Corresponding Author:
Moriah L. Szpara
Dept. of Biochemistry & Molecular Biology
The Huck Institutes of the Life Sciences
W-208 Millennium Science Complex (MSC)
Pennsylvania State University
University Park, PA 16802 USA
Phone: 814-867-0008
Email: moriah@psu.edu

Author emails:
Christopher D. Bowen: cdb5004@psu.edu
Henrik Paavilainen: hojpaa@utu.fi
Daniel W. Renner: dwr19@psu.edu
Jussi Palomäki: jmmpal@utu.fi
Jenni Lehtinen: jenni.lehtinen@bayer.com
Tytti Vuorinen: tyvuori@utu.fi
Peter Norberg: peter.norberg@microbio.gu.se
Veijo Hukkanen: veijo.hukkanen@utu.fi
Moriah L. Szpara: moriah@psu.edu

Abstract

A majority of adults in Finland are seropositive carriers of herpes simplex viruses (HSV). Infection occurs at epithelial or mucosal surfaces, after which virions enter innervating nerve endings, eventually establishing lifelong infection in neurons of the sensory or autonomic nervous system. Recent data have highlighted the genetic diversity of HSV-1 strains, and demonstrated apparent geographic patterns in strain similarity. Though multiple HSV-1 genomes have been sequenced from Europe to date, there is a dearth of sequenced genomes from Nordic countries. Finland's history includes at least two major waves of human migration, suggesting the potential for diverse viruses to persist in the population. Here we used HSV-1 clinical isolates from Finland to test the relationship between viral phylogeny, genetic variation, and phenotypic characteristics. We found that Finnish HSV-1 isolates separated into two distinct phylogenetic groups, potentially reflecting the two historical waves of human (and viral) migration into Finland. The amount of genetic diversity found in these ten clinical isolates was similar to that found between independent HSV-1 strains from other geographic areas. These HSV-1 isolates harbored distinct phenotypes in cell culture, including differences in virus production, extracellular virus release, and cell-type-specific fitness. Importantly, these phenotypic differences did not partition into the same groups as the phylogenetic clusters, demonstrating that whole-genome relatedness is not a proxy for overall viral phenotype. Instead, we highlight specific gene-level differences that may contribute to observed phenotypic differences, and we note that strains from different phylogenetic groups have converged to achieve the same genetic variations.

Keywords: Herpes simplex virus (HSV), comparative genomics, phylogeny, genotype, phenotype, genetic variation

61 # Introduction

62 Human herpes simplex virus 1 (HSV-1; Family: *Herpesviridae,* Genus: *Simplexvirus,* species:
63 *Human herpesvirus 1*) has been recognized as a major human malady since the era of
64 Hippocrates (1), and to this day there is no effective vaccine (2). Approximately 50% of adults in
65 Finland are seropositive for HSV-1 (3–5), and 13% are seropositive for HSV-2 (3, 6). HSV
66 infects via epithelial or mucosal surfaces, after which it is taken up by nerve endings and
67 establishes a lifelong infection in neurons of the sensory or sympathetic nervous system. From
68 these neuronal sites the virus can reactivate, transit via nerve endings back to the skin surface,
69 and re-initiate skin or mucosal shedding at the same site as the original infection. In addition to
70 recurrent epithelial lesions, HSV also causes infectious keratitis, worsens acquisition and
71 shedding rates for human immunodeficiency virus (HIV), and can progress to cause rare but life-
72 threatening encephalitis (1).

73 Recent comparative genomics studies of HSV-1, from our lab and others, have demonstrated that
74 HSV-1 strains from unrelated individuals can differ in 2-4% of the viral genome (7–13). HSV-1
75 has a large DNA genome of ~152 kilobases, encoding >75 proteins (14, 15). Sequence-based
76 comparisons of HSV-1 strains have demonstrated at least three major clades (16, 17), with
77 evidence of geographic clustering (9, 18), as well as recombination between these groups. HSV-
78 1 displays greater host-to-host variation than any other alpha-herpesvirus (9, 19): approximately
79 double the amount found in HSV-2 (20, 21), and 5-fold higher than found between isolates of
80 varicella zoster virus (VZV) (22–24). The impacts of these naturally occurring viral genetic
81 variations on virulence and pathogenesis in humans are unknown. Examining the phenotypic
82 differences displayed by HSV-1 strains in culture provides an opportunity to explore the scope of

83 these differences and test whether or not they are linked to previously observed patterns of
84 geographic diversity.

85 Finland has a unique history that has led to a relatively homogeneous and stable population,
86 providing a unique view on the evolution of viruses that are persistent in the population. There
87 have been two major migratory sweeps contributing to expansion of the human population of
88 Finland: the first wave from the east, occurring ca. 4000 years ago, and another wave from the
89 south (southwest) ca. 2000 years ago (25–27). Finland also has one of the best genealogical
90 databases in the world, which in combination with computerized medical records and a high rate
91 of patient participation, has led to many recent advances in human medical genetics (28, 29).
92 This may enable future studies to explore the co-evolution of human and viral genetic variation
93 in this population.

94 We have characterized ten HSV-1 strains isolated from a random subset of Finland clinic visits,
95 and compared their growth properties, drug resistance, and other phenotypic features. Full
96 genome sequences of these viruses were compared to each other and to other previously
97 described strains of HSV-1, to reveal patterns of inter-host and intra-host variability. We found
98 that the observed phenotypic differences did not partition into the same sub-groups as the overall
99 genomic patterns, demonstrating that whole-genome relatedness is not a proxy for viral
100 phenotype. We anticipate that these data will aid in efforts to develop improved sequence-based
101 antiviral therapies and contribute to development of a vaccine against HSV infections (30).
102 These data present an opportunity to explore the diversity of chronic herpesviruses in the Finland
103 population, and to lay the foundation for future studies that explore the connections between

104 viral genetic differences, host genetic predispositions, and their potential relationship(s) to
105 clinical outcomes of HSV-1 infection.

106

107 # Methods

108 **Virus isolates and virus stock propagation**

109 Clinical isolates were obtained from anonymous coded diagnostic samples from herpes lesions
110 representing currently circulating viral strains in Finland (**Table 1**). Approval for the study of
111 anonymous HSV isolates was provided by the Turku University Central Hospital (permit #
112 J10/17).

113 An immunoperoxidase-rapid culture assay (31) was used to type the viruses as HSV-1, which
114 was confirmed by a HSV type-specific gD (US6) gene-based PCR test (32). Viruses were
115 initially propagated on Vero cells (African green monkey kidney cells; ATCC), maintained in
116 Dulbecco's MEM with 2% fetal calf serum and gentamycin. A stock was made by addition of 3
117 ml of 9% autoclaved skimmed milk (Valio, Finland) on to 5 ml of the culture medium and
118 subsequent freezing. The cells and the medium were collected and combined upon thawing, and
119 were frozen and thawed for two further rounds before aliquoting. The viral titer was determined
120 by plaque titration on Vero cells as described before (33). Parallel aliquots were used for further
121 viral culture studies and for preparation of viral nucleocapsid DNA. For viral production data,
122 SPSS Statistics 20 (IBM, Armonk NY, USA) software was use to perform statistical analyses.
123 Non-parametric Mann-Whitney U-test was used to calculate statistical significances. The
124 threshold for significance was set to $p<0.05$.

125 **Viral genomic DNA isolation**

126 The viral genomic DNA was prepared from isolated viral nucleocapsids as described previously
127 (7, 34). In brief, viral stock collected from the first or second passage in Vero cells was used to
128 infect ~$1x10^8$ HaCaT cells (Department of Dentistry, University of Turku (35)) at a multiplicity
129 of infection (m.o.i.) of 0.1-1 plaque-forming units (PFU)/cell, and the infection was allowed to
130 proceed to completion at +35 °C (1-3 days). The cells were collected, washed with PBS and
131 suspended to LCM buffer (0.125 M KCl, 30 mM Tris pH 7.4, 5 mM $MgCl_2$, 0.5 mM EDTA,
132 0.5% Nonidet P-40; with 0.6 mM beta-mercaptoethanol). After two successive extractions with
133 Freon (1,1,2-trichloro-1,2,2-trifluoroethane, Sigma-Aldrich), the extracts were added on top of
134 layers in LCM buffer with 45% and 5% glycerol and ultracentrifuged at 77 000 x g for 1 h at
135 +4ºC (Beckman Coulter SW41Ti rotor). Viral nucleocapsids were recovered from the bottom of
136 the ultracentrifuge tube, and the DNA was prepared by treatment with Proteinase K and SDS,
137 followed by repeated extractions with phenol-chloroform and ethanol precipitation. The DNA
138 content and purity were observed by spectrophotometry and by agarose gel electrophoresis after
139 restriction enzyme digestions.

140 **Cell culture**

141 Vero cells (ATCC; Manassas, VA) were propagated in M199 medium supplemented with 5%
142 fetal bovine serum and gentamycin. HaCaT cells (Department of Dentistry, University of Turku;
143 (35)) were propagated in DMEM medium with HEPES buffer, supplemented with 7% fetal
144 bovine serum and gentamycin. SH-SY5Y neuroblastoma cells (K. Åkerman, Åbo Akademi
145 University, Turku, Finland) were propagated in DMEM (high glucose) medium supplemented
146 with 10% fetal bovine serum, 2 mM L-glutamine and gentamycin. Initial differentiation of SH-

147 SY5Y cells involved culture for 10 days in DMEM/F-12 medium containing 5% fetal bovine
148 serum, 10 μM All-trans retinoic acid (Sigma), 2 mM L-glutamine and gentamycin. Thereafter
149 SH-SY5Y cells were transferred on Matrigel-coated (B-D) 96-well plates and the medium was
150 changed to serum-free DMEM/F-12 medium containing 10 μM all-trans retinoic acid (Sigma),
151 0.5 μg/ml of brain-derived neurotrophic factor (Millipore), 2 mM L-glutamine and gentamycin.

152 **Acyclovir resistance testing**

153 The sensitivity of each HSV strain to acyclovir was tested in a microplate format. Vero cells
154 grown on 96-well cell culture plates were treated with cell culture medium (DMEM with 5%
155 fetal bovine serum) supplemented with acyclovir (ACV; Sigma), in concentrations of 128 μg/ml
156 to 0.03125 μg/ml (1:4 serial dilutions). Duplicate wells containing each ACV dilution, and wells
157 without ACV, were infected with 100 PFU of each virus. As a control, the HSV-1 delta305 virus
158 was included; it is resistant to ACV due to deletion of its thymidine kinase gene (36). Infected
159 cells were incubated at +37°C, at 5% CO_2, for 72 hours before fixation with methanol and
160 staining with crystal violet. The reduction of plaque numbers at each ACV dilution was observed
161 in comparison with wells infected without ACV. A logistic fit curve was used for determination
162 of IC_{50} values. A virus with an IC_{50} value of over 2 μg/ml (of ACV) was considered resistant
163 (37).

164 **Image acquisition**

165 Photomicrographic images of viral plaques were obtained using a Zeiss Primovert inverted
166 microscope with Plan-Achromat 4x and 10x objectives, recorded using an AxioCam ERc 5s
167 camera, and analyzed using Zeiss ZEN 2012 software.

168 **Next generation sequencing**

169 Viral nucleocapsid DNA was sheared on a Covaris M220 (parameters: 60 seconds duration, peak
170 power 50, 10% duty cycle, 4C). We used the Illumina TruSeq DNA Sample Prep kit to prepare
171 barcoded sequencing libraries, according to the manufacturer's protocol for low-throughput
172 sample handling. Libraries were quantified and assessed by Qubit (Invitrogen, CA), Bioanalyzer
173 (Agilent), and library adapter qPCR (KAPA Biosystems). Illumina MiSeq paired-end sequencing
174 (2 x 300 bp) was completed according to manufacturer's recommendations, using 17 pM library
175 concentration.

176 A consensus viral genome for each strain was assembled using a *de novo* viral genome assembly
177 (VirGA) workflow (10). This approach begins with quality control, including removal of
178 contaminating host sequences, adapters from library preparation, and imaging artifacts. Next
179 VirGA iterates through multiple *de novo* assemblies using SSAKE, which we then combine into
180 longer blocks of sequence (contigs) using Celera and GapFiller. VirGA uses Mugsy alignment to
181 match these contigs to the HSV-1 reference genome (strain 17, GenBank accession JN555585).
182 The best-matched contigs are stitched into a single consensus genome, which is then annotated
183 and subjected to additional quality control measures. These include an examination of coverage
184 (sequence read) depth, detection of minority variants within each consensus genome, and manual
185 inspection of gaps and low coverage areas. See **Table 2** for GenBank accessions.

186 **Intra-strain minority-variant detection**

187 Minority-variant (MV) positions within each *de novo* assembled genome were determined using
188 VarScan v2.2.11 as previously described (38, 39). Conservative variant calling parameters to

189 eliminate sequencing-induced errors were set at: minimum allele frequency ≥0.02; base call
190 quality ≥20; read depth at the position ≥100; independent reads supporting minor allele ≥5. MVs
191 containing ≥90% unidirectional strand support were excluded from further analyses (40, 41).
192 MVs passing quality control were mapped to respective genomes and assessed for mutational
193 effect using SnpEff and SnpSift (42, 43).

194 **Phylogenetic and recombination analyses**

195 DNA sequences were aligned using the Kalign algorithm included in eBioTools. To avoid
196 inferences caused by false phylogenetic signals, all gap and repeat regions were excluded prior to
197 this analysis. Repeat regions not leading to gaps were also excluded since these may contain
198 single nucleotide differences that have been shuffled into new positions by random aspects of
199 tandem-repeat alignment. Furthermore, ambiguous nucleotides that were marked as "N" were
200 excluded, along with the corresponding aligned nucleotides in remaining sequences. Complete
201 genomes in GenBank harbouring long stretches of "N" were not included in the analysis (e.g.
202 strain B3x_1_5). In total, 110,168 nucleotides were analysed in each genome.

203 The phylogenetic network was constructed by using SplitsTree4. It is a NeighborNet with
204 OrdinaryLeastSquares Variance depicted as a RootedEqualAngle splits tree. A recombination
205 test on the complete dataset was performed by using the Phi test for recombination implemented
206 in SplitsTree4.

207 **Restriction fragment length polymorphism (RFLP) analysis**

208 A cytoplasmic viral DNA preparation was modified from the protocol described by Igarashi et al
209 (44). Subconfluent Vero cell cultures were infected at an m.o.i of 0.1, and incubated at +34ºC for

210 2 days until the cytopathic effect was complete. The cells were collected in 150 mM NaCl, 10
211 mM Tris pH 7.6, 1.5 mM MgCl buffer, with 0.1% Nonidet P-40. The nuclei were pelleted, and
212 DNA was extracted from the supernatant by two successive extractions with phenol-chloroform.
213 DNA was recovered by ethanol precipitation. 12.5 µg of each viral DNA was diluted in 15 µl
214 solution containing sterile H_2O, FastDigest 10X green buffer and FastDigest BamHI or SalI
215 restriction enzyme (Thermo Scientific). Electrophoresis was run in 0.8 % TBE-agarose gels, with
216 GeneRuler mix DNA ladder, for 24 h at 45 V before imaging. In order to separate large DNA
217 fragments after SalI digestion, electrophoresis was continued for additional 36 h at 30 V.

218

219 Results

220 Comparison of growth properties of Finnish HSV-1 strains in vitro

221 A random set of ten circulating Finnish HSV-1 isolates were selected from residual laboratory
222 diagnostic specimens (**Table 1)**. We first examined *in vitro* phenotypic characteristics of these
223 HSV-1 isolates, by comparing their overall titer and rate of intracellular virus vs. extracellular
224 (released) virus production at 24 hours post infection (hpi) of a range of cell types (**Figure 1**).
225 These included non-human primate kidney-derived epithelial (Vero) cells (**Figure 1A**), human
226 keratinocyte (HaCaT) cells (**Figure 1B**), and human neuroblastoma (SH-SY5Y) cells in a mixed,
227 undifferentiated state (**Figure 1C**), as well as a differentiated, neuronal state (**Figure 1D**).
228 Compared to epithelial and keratinocyte cells, overall viral production was markedly reduced in
229 neuronal precursor cells and differentiated neuronal cells (compare **Figure 1AB** vs. **CD**). The
230 wild-type HSV-1 reference strain 17+ replicated to significantly higher titers than any of the

231 circulating clinical isolates in Vero cells, which are standardly used for HSV propagation, and to
232 a lesser extent strain 17+ replicated at higher titer in other cell types as well (**Figure 1**; $p<0.05$,
233 10-100 fold higher viral amounts). Different clinical isolates excelled at producing virions in
234 each cell type, with no clear patterns of most- or least-efficient viral production or release across
235 all cell types. The amount of extracellular released virus was less than 10% of the total virion
236 production, in all cell types except the undifferentiated neuronal precursor cells (**Supplemental**
237 **Figure S1**). Each virus strain was also tested for acyclovir (ACV) resistance. Despite some
238 variation in ACV susceptibility (IC50 values), none of the circulating Finnish viruses was
239 considered resistant to ACV (**Table 1**). There were also no significant differences among the 10
240 clinical isolates in the plaque morphology or the type of cytopathic effect induced in Vero cell
241 cultures (**Figure 2**).

242 **Genetic and genomic analysis of Finnish HSV-1 strains**

243 Based on prior data suggesting the effects of successive waves of migration on the human
244 population in Finland (25, 26), we next assessed the overall genetic diversity of these ten HSV-1
245 isolates. We first performed a restriction fragment length polymorphism (RFLP) analysis on viral
246 genomic DNA, which revealed at least two broad patterns of variation (**Figure 3** and
247 **Supplemental Figure S2**). The diversity of bands led us to examine these genetic differences
248 with greater precision using high-throughput, deep genome sequencing (HTS) and comparative
249 genomics analysis (see **Methods** for details). A previously described bioinformatics pipeline was
250 used to *de novo* assemble a full-length consensus genome for each strain **(Table 2)**. A viral
251 consensus genome represents the most common nucleotide detected at each nucleotide position
252 in that viral population. All viral genomes had a coverage depth between 1,000-2,800-fold, with

253 >96% of the genome covered at a depth exceeding 100-fold **(Table 2)**. This depth enabled us to
254 compare the full genetic complement of the viral genome for each strain, and to analyze
255 differences both between and within each viral strain population, and to compare them to
256 previously described viral genomes.

257 Genetic relatedness of Finland HSV-1 samples

258 First, we used the viral consensus genomes to compare how overall variation in these ten Finnish
259 HSV-1 genomes related to the patterns observed by RFLP analysis (**Figure 3**). Whole genome
260 alignments were created using the ten Finnish HSV-1 genomes, as well as these ten in
261 conjunction with a diverse set of previously published HSV-1 genomes (see Methods and
262 **Supplemental Table S1** for a full list). We then used SplitsTree to create a network graph that
263 revealed the relatedness of the ten Finnish viral genomes to each other (**Figure 4A**) and to
264 previously described HSV-1 genomes (**Figure 4B**). This approach revealed that the Finland
265 HSV-1 genomes separated into two sub-groups, which appear to relate to previously recognized
266 Asian and European / North American clades. These data echo those of the initial RFLP analysis.

267 Protein-coding variation in Finland HSV-1 samples

268 Next, we examined more fine-scale genetic differences in these HSV-1 isolates, which are
269 invisible at the level of RFLP analysis. Here we examined DNA- and amino acid (AA)-
270 alignments for each protein-coding region of the HSV-1 genome (**Supplemental Table S2-S3**).
271 We found that from zero to 8% of each coding region differed at the AA level between the ten
272 Finnish viral genomes (**Figure 5**). Only a handful of small coding regions (UL20, VP26 (UL35),
273 UL49A, UL55) showed no AA variation at all between viral isolates. Consistent with previous

274 findings (9), gL (UL1), UL11, UL43, gG (US4), and gJ (US5) were among the most divergent
275 proteins. Together these inter-strain genetic differences in 70 HSV-1 proteins in **Figure 5**
276 provide ample opportunities to generate the phenotypic diversity observed in **Figure 1**. Overall,
277 these levels of AA coding diversity reflect those seen in previous analyses (9), and between other
278 known HSV-1 genomes.

279 **Minority allelic variants in Finland HSV-1 viral populations**

280 Each viral consensus genome represents the most common nucleotide detected at each position
281 in the viral genome. In contrast, minority variants (MV) within each viral population are rare
282 alleles, presented in <50% of the sequenced reads. These MV may rise to greater prevalence
283 during viral spread to new niches or hosts, or under selective evolutionary pressure. For each
284 viral genome, we examined the number of MVs detected in each genome. Stringent quality-
285 control criteria were used to reduce the number of false-positive MVs (see **Methods**), such that
286 only those MV detected at ≥2% prevalence were used in this analysis. MVs were found
287 dispersed across each genome (**Supplemental Figure S3**), mostly in intergenic regions. A
288 concentration of MVs were found near tandem repeats in VP1/2 (UL36), gI (US7), and in the
289 internal-repeat regions, which may result from stochasticity in tandem repeat alignment in these
290 regions. The MVs detected in gI occur at the same tandem-repeat site as the consensus-level AA
291 variations in this gene (**Figure 6**). Taken together, these results define the level of inter-host
292 (**Figure 5**) and intra-host (**Supplemental Figure S3**) variation seen in the Finnish HSV-1 strains
293 described herein.

294 **Patterns of variation in Finnish HSV-1 strains**

295 Finally, we considered whether any of the observed patterns of genomic or phenotypic variation
296 could be linked to fine-scale coding variations in these ten Finnish HSV-1 isolates. The genomic
297 sub-groups detected by RFLP (**Figure 3**) and network graph analysis (**Figure 4**) were reflected
298 in several coding variations that correlated with phylogenetic group. For example, coding
299 differences in the secreted and virion surface glycoprotein G (gG; US4) correlated with the two
300 Finnish phylogenetic sub-groups (**Figure 6A**; see **Figure 4** for phylogenetic sub-groups). Other
301 impacts on coding variation may result from changes in copy number at tandem repeats.
302 Variation in tandem repeat length in glycoprotein I (gI; US7) leads to expansion of a repeating
303 tract of mucin-type O-linked glycosylation sites (**Figure 6B)**, akin to that previously described in
304 clinical isolates of HSV-1 (16, 45). Finally, there are detectable patterns of AA variation that
305 correlate with phenotypic differences in viral fitness in specific cell types. Coding differences in
306 the nuclear egress complex protein NEC2 (UL34) (**Figure 6C**) were observed in the two strains
307 (F-12g, M-15) which showed no detectable extracellular virion release in differentiated neuronal
308 cells (**Figure 1D**). The terminally differentiated and non-dividing state of these neuronal cells
309 may constitute a sensitized background to detect impacts on virion egress. Taken together, these
310 examples illustrate the type and degree of variation present in these strains, and highlight
311 potential genetic insights into viral phenotype.

312

313 # Discussion

314 In this study, we described the first-ever HSV-1 genomes from Finland. Two distinct sub-groups
315 or clades were observed in the ten Finnish clinical isolates, with four strains clustering in one
316 clade and six in another. These groups were detectable using both classical RFLP approaches
317 (**Figure 3**) and deep-sequencing methods for whole-genome analyses (**Figure 4**). These data
318 appear to corroborate previous findings that show multiple colonization events of Finland, with
319 migration from Europe in the south and Asia in the northeast (25, 26). However, we found that
320 phenotypic differences between these isolates were uncoupled from the overall genomic patterns
321 that grouped them into two geographic clades. While plaque morphology was consistent across
322 isolates (**Figure 2**), the amount of virus production, extracellular virion release, and acyclovir
323 sensitivity differed between isolates and across cell types (**Figure 1** and **Table 1**). We detected
324 gene-specific patterns of genetic variation that may well impact protein function. Future studies
325 will need to dissect individual genetic variations in each viral isolate in order to test their precise
326 impact(s) on viral fitness.

327 When analyzing the replication capabilities of these recently isolated clinical samples in multiple
328 cell types, we found that they replicated to lower overall titers and produced fewer extracellular
329 virions than the lab-adapted HSV-1 strain 17+, regardless of cell type (**Figure 1** and
330 **Supplemental Figure S1**). This difference was more pronounced in non-human primate and
331 human epithelial cells, and was more subtle in neuronal precursors and differentiated neuronal
332 cells. There did not appear to be any clear differences in titer or extracellular virus production
333 between geographic clades. There also seemed to be no noticeable differences in plaque
334 morphology among these samples, with plaque size and cellular cytopathic effect being similar

335 across all samples. Although we report findings in a number of cell lines in this study, it will be
336 important for future studies to examine each virus and cell-type pairing separately, since these
337 data demonstrate that maximal viral fitness in one cell type is not generally predictive of fitness
338 in another.

339 We observed several potential connections between genetic differences and phenotypic
340 differences. For instance, we detected an AA difference in the UL34 (NEC2) binding domain in
341 F-12g and M-15 **(Figure 6C).** Previous work has shown that the viral proteins UL31 (NEC1) and
342 UL34 (NEC2) form a nuclear egress complex that localizes to the perinuclear space and plays a
343 critical role in egress of viral capsids from the nucleus (46, 47). In these two clinical isolates (F-
344 12g and M-15), there was no measurable amount of extracellular virus produced in differentiated
345 neuronal cells (**Figure 1D**). Further studies will be needed to examine if this phenotype is linked
346 to a disruption of NEC1 and NEC2 binding and impaired nuclear egress for isolates F-12g and
347 M-15. Variation in the copy-number of tandem repeats is yet another way that HSV-1 isolates
348 can generate genetic and potential phenotypic variation. Glycoprotein I (gI; US7) contains a
349 mucin-like domain with repeating units of serine, threonine, and proline (**Figure 6B**). This
350 domain varies in length across these isolates. This domain has been previously shown to serve as
351 a site of O-linked glycosylation, with longer tracts (e.g. 8 repeating units) being more heavily
352 glycosylated than short tracts (e.g. 2 repeating units) (16, 45). A prior study of over 80 Swedish
353 HSV-1 isolates found that the vast majority of isolates (>75%) had four or fewer repeating units
354 in this gI domain (16, 45). In contrast, more than half of the Finland HSV-1 isoaltes analyzed
355 here have 8 or more repeating units, suggesting that their gI proteins may be more heavily

356 glycosylated in this domain. These data generate hypotheses for future investigations of
357 genotype-phenotype links in these and other new clinical isolates.

358 This study provides one of the first combinations of phenotypic analyses that span multiple cell
359 types, alongside full comparative genomic analyses that span both phylogenetic and gene-
360 specific analyses. One comparison not yet explored in this or prior studies is the specific pairing
361 of each virus with cells derived from the human source of each isolate. This approach is now
362 technically feasible, using induced pluripotent stem cell technology to generate specific cell
363 types from a single source such as a buccal swab. The rich genealogical databases in Finland
364 suggest an opportunity to not only pair these analyses at the human-cell and virus level, but also
365 to link observed phenotypes of cellular infection to each patient's clinical and/or familial history
366 of herpesvirus disease. We anticipate that in the future, this approach would yield fruitful
367 insights not only into direct clinical outcomes of herpesvirus disease, but also generate
368 hypotheses about herpesvirus co-morbidities.

369

370 Acknowledgements

371 The authors thank members of the Hukkanen and Szpara labs for helpful feedback and
372 discussion. We acknowledge Ritva Kajander for preparation of the viral stocks and the viral
373 nucleocapsid DNA. This work was supported by research startup funds (MLS) from the
374 Pennsylvania State University, and by a grant from the Pennsylvania Department of Health using
375 CURE funds (MLS). The Department specifically disclaims responsibility for any analyses,
376 interpretations, or conclusions. The funding from the Jane and Aatos Erkko Foundation grant

377 #170046 is acknowledged. We thank Prof. Bernard Roizman, University of Chicago, for the
378 delta305 virus.

379

380 # References

381 1. Roizman B, Sears E. 1996. Herpes simplex viruses and their replication, p. 1043–1107. *In*
382 Fields, BN, Knipe, DM, Howley, PM (eds.), Fundamental virology, 3rd ed. Lippincott-
383 Raven, Philadelphia, PA.

384 2. Johnston C, Koelle DM, Wald A. 2011. HSV-2 : in pursuit of a vaccine. J Clin Invest
385 121:4600–4609.

386 3. Pebody RG. 2004. The seroepidemiology of herpes simplex virus type 1 and 2 in Europe.
387 Sex Transm Infect 80:185–191.

388 4. Puhakka L, Sarvikivi E, Lappalainen M, Surcel H-M, Saxen H. 2016. Decrease in
389 seroprevalence for herpesviruses among pregnant women in Finland: cross-sectional study
390 of three time points 1992, 2002 and 2012. Infect Dis 48:406–410.

391 5. Looker KJ, Magaret AS, May MT, Turner KME, Vickerman P, Gottlieb SL, Newman LM.
392 2015. Global and regional estimates of prevalent and incident herpes simplex virus type 1
393 infections in 2012. PLoS ONE 10:e0140765.

394 6. Looker KJ, Magaret AS, Turner KME, Vickerman P, Gottlieb SL, Newman LM. 2015.
395 Global estimates of prevalent and incident herpes simplex virus type 2 infections in 2012.
396 PloS One 10:e114989.

397 7. Szpara ML, Parsons L, Enquist LW. 2010. Sequence variability in clinical and laboratory
398 isolates of herpes simplex virus 1 reveals new mutations. J Virol 84:5303–13.

399 8. Kolb AW, Adams M, Cabot EL, Craven M, Brandt CR. 2011. Multiplex sequencing of seven
400 ocular herpes simplex virus type-1 genomes: phylogeny, sequence variability, and SNP
401 distribution. Invest Ophthalmol Vis Sci 52:9061–73.

402 9. Szpara ML, Gatherer D, Ochoa A, Greenbaum B, Dolan A, Bowden RJ, Enquist LW,
403 Legendre M, Davison AJ. 2014. Evolution and diversity in human herpes simplex virus
404 genomes. J Virol 88:1209–27.

405 10. Parsons LR, Tafuri YR, Shreve JT, Bowen CD, Shipley MM, Enquist LW, Szpara ML.
406 2015. Rapid genome assembly and comparison decode intrastrain variation in human
407 alphaherpesviruses. mBio 6:e02213-14.

408 11. Bowen CD, Renner DW, Shreve JT, Tafuri Y, Payne KM, Dix RD, Kinchington PR,
409 Gatherer D, Szpara ML. 2016. Viral forensic genomics reveals the relatedness of classic
410 herpes simplex virus strains KOS, KOS63, and KOS79. Virology 492:179–186.

411 12. Pfaff F, Groth M, Sauerbrei A, Zell R. 2016. Genotyping of herpes simplex virus type 1
412 (HSV-1) by whole genome sequencing. J Gen Virol.

413 13. Greninger AL, Roychoudhury P, Xie H, Casto A, Cent A, Pepper G, Koelle DM, Huang M-
414 L, Wald A, Johnston C, Jerome KR. 2018. Ultrasensitive Capture of Human Herpes
415 Simplex Virus Genomes Directly from Clinical Samples Reveals Extraordinarily Limited
416 Evolution in Cell Culture 3:12.

417 14. Davison AJ. 2012. Evolution of sexually transmitted and sexually transmissible human
418 herpesviruses. Ann N Y Acad Sci 1230:E37–E49.

419 15. Roizman B, Knipe DM, Whitley R. 2013. Herpes Simplex Viruses, p. 1823–1897. *In* Fields
420 Virology, 6th ed. Lippincott Williams & Wilkins, Philadelphia, PA.

421 16. Norberg P, Bergstrom T, Rekabdar E, Lindh M. 2004. Phylogenetic Analysis of Clinical
422 Herpes Simplex Virus Type 1 Isolates Identified Three Genetic Groups and Recombinant
423 Viruses. J Virol 78:10755–10764.

424 17. Norberg P. 2010. Divergence and genotyping of human alpha-herpesviruses: an overview.
425 Infect Genet Evol J Mol Epidemiol Evol Genet Infect Dis 10:14–25.

426 18. Kolb AW, Ané C, Brandt CR. 2013. Using HSV-1 genome phylogenetics to track past
427 human migrations. PloS One 8:1–9.

428 19. Sijmons S, Thys K, Mbong Ngwese M, Van Damme E, Dvorak J, Van Loock M, Li G,
429 Tachezy R, Busson L, Aerssens J, Van Ranst M, Maes P. 2015. High-Throughput Analysis
430 of Human Cytomegalovirus Genome Diversity Highlights the Widespread Occurrence of
431 Gene-Disrupting Mutations and Pervasive Recombination. J Virol 89:7673–7695.

432 20. Newman RM, Lamers SL, Weiner B, Ray SC, Colgrove RC, Diaz F, Jing L, Wang K, Saif S,
433 Young S, Henn M, Laeyendecker O, Tobian AAR, Cohen JI, Koelle DM, Quinn TC, Knipe
434 DM. 2015. Genome Sequencing and Analysis of Geographically Diverse Clinical Isolates
435 of Herpes Simplex Virus 2. J Virol JVI.01303-15.

436 21. Kolb AW, Larsen IV, Cuellar JA, Brandt CR. 2015. Genomic, Phylogenetic, and
437 Recombinational Characterization of Herpes Simplex Virus 2 Strains. J Virol 89:6427–
438 6434.

439 22. Tyler SD, Peters GA, Grose C, Severini A, Gray MJ, Upton C, Tipples GA. 2007. Genomic
440 cartography of varicella-zoster virus: a complete genome-based analysis of strain variability
441 with implications for attenuation and phenotypic differences. Virology 359:447–58.

442 23. Zell R, Taudien S, Pfaff F, Wutzler P, Platzer M, Sauerbrei A. 2012. Sequencing of 21
443 Varicella-Zoster Virus Genomes Reveals Two Novel Genotypes and Evidence of
444 Recombination. J Virol 86:1608–1622.

445 24. Depledge DP, Gray ER, Kundu S, Cooray S, Poulsen A, Aaby P, Breuer J. 2014. Evolution
446 of Cocirculating Varicella-Zoster Virus Genotypes during a Chickenpox Outbreak in
447 Guinea-Bissau. J Virol 88:13936–13946.

448 25. Kittles RA, Perola M, Peltonen L, Bergen AW, Aragon RA, Virkkunen M, Linnoila M,
449 Goldman D, Long JC. 1998. Dual Origins of Finns Revealed by Y Chromosome Haplotype
450 Variation. Am J Hum Genet 62:1171–1179.

451 26. Varilo T, Paunio T, Parker A, Perola M, Meyer J, Terwilliger JD, Peltonen L. 2003. The
452 interval of linkage disequilibrium (LD) detected with microsatellite and SNP markers in
453 chromosomes of Finnish populations with different histories. Hum Mol Genet 12:51–59.

454 27. Lappalainen T, Laitinen V, Salmela E, Andersen P, Huoponen K, Savontaus M-L, Lahermo
455 P. 2008. Migration Waves to the Baltic Sea Region. Ann Hum Genet 72:337–348.

456 28. Hannelius U, Salmela E, Lappalainen T, Guillot G, Lindgren CM, von Döbeln U, Lahermo
457 P, Kere J. 2008. Population substructure in Finland and Sweden revealed by the use of
458 spatial coordinates and a small number of unlinked autosomal SNPs. BMC Genet 9:54.

459 29. Ilonen J, Reijonen H, Green A, Reunanen A, Knip M, Simell O, Akerblom HK. 2000.
460 Geographical differences within Finland in the frequency of HLA-DQ genotypes associated
461 with type 1 diabetes susceptibility. The Childhood Diabetes in Finland Study Group. Eur J
462 Immunogenetics Off J Br Soc Histocompat Immunogenetics 27:225–230.

463 30. Paavilainen H, Lehtinen J, Romanovskaya A, Nygårdas M, Bamford DH, Poranen MM,
464 Hukkanen V. 2016. Inhibition of clinical pathogenic herpes simplex virus 1 strains with
465 enzymatically created siRNA pools: siRNA Pools Against Clinical HSV Strains. J Med
466 Virol 88:2196–2205.

467 31. Ziegler T, Waris M, Rautiainen M, Arstila P. 1988. Herpes simplex virus detection by
468 macroscopic reading after overnight incubation and immunoperoxidase staining. J Clin
469 Microbiol 26:2013–2017.

470 32. Hukkanen V, Rehn T, Kajander R, Sjöroos M, Waris M. 2000. Time-resolved fluorometry
471 PCR assay for rapid detection of herpes simplex virus in cerebrospinal fluid. J Clin
472 Microbiol 38:3214–3218.

473 33. Romanovskaya A, Paavilainen H, Nygårdas M, Bamford DH, Hukkanen V, Poranen MM.
474 2012. Enzymatically produced pools of canonical and Dicer-substrate siRNA molecules

475 display comparable gene silencing and antiviral activities against herpes simplex virus.
476 PloS One 7:e51019.

477 34. Szpara ML, Tafuri YR, Enquist LW. 2011. Preparation of viral DNA from nucleocapsids. J
478 Vis Exp JoVE 2–7.

479 35. Boukamp P, Petrussevska RT, Breitkreutz D, Hornung J, Markham A, Fusenig NE. 1988.
480 Normal keratinization in a spontaneously immortalized aneuploid human keratinocyte cell
481 line. J Cell Biol 106:761–771.

482 36. Post LE, Mackem S, Roizman B. 1981. Regulation of alpha genes of herpes simplex virus:
483 expression of chimeric genes produced by fusion of thymidine kinase with alpha gene
484 promoters. Cell 24:555–565.

485 37. Tardif KD, Jorgensen S, Langer J, Prichard M, Schlaberg R. 2014. Simultaneous titration
486 and phenotypic antiviral drug susceptibility testing for herpes simplex virus 1 and 2. J Clin
487 Virol 61:382–386.

488 38. Koboldt DC, Zhang Q, Larson DE, Shen D, McLellan MD, Lin L, Miller CA, Mardis ER,
489 Ding L, Wilson RK. 2012. VarScan 2: Somatic mutation and copy number alteration
490 discovery in cancer by exome sequencing. Genome Res 22:568–576.

491 39. Pandey U, Renner DW, Thompson RL, Szpara ML, Sawtell NM. 2017. Inferred father-to-
492 son transmission of herpes simplex virus results in near-perfect preservation of viral
493 genome identity and in vivo phenotypes. Sci Rep 7:13666.

494 40. Nakamura K, Oshima T, Morimoto T, Ikeda S, Yoshikawa H, Shiwa Y, Ishikawa S, Linak
495 MC, Hirai A, Takahashi H, Altaf-Ul-Amin M, Ogasawara N, Kanaya S. 2011. Sequence-
496 specific error profile of Illumina sequencers. Nucleic Acids Res 39:1–13.

497 41. Depledge DP, Kundu S, Jensen NJ, Gray ER, Jones M, Steinberg S, Gershon A, Kinchington
498 PR, Schmid DS, Balloux F, Nichols RA, Breuer J. 2014. Deep Sequencing of Viral
499 Genomes Provides Insight into the Evolution and Pathogenesis of Varicella Zoster Virus
500 and Its Vaccine in Humans. Mol Biol Evol 31:397–409.

501 42. Cingolani P, Platts A, Wang LL, Coon M, Nguyen T, Wang L, Land SJ, Lu X, Ruden DM.
502 2012. A program for annotating and predicting the effects of single nucleotide
503 polymorphisms, SnpEff. Fly (Austin) 6:80–92.

504 43. Cingolani P, Patel VM, Coon M, Nguyen T, Land SJ, Ruden DM, Lu X. 2012. Using
505 Drosophila melanogaster as a Model for Genotoxic Chemical Mutational Studies with a
506 New Program, SnpSift. Front Genet 3.

507 44. Igarashi K, Fawl R, Roller RJ, Roizman B. 1993. Construction and properties of a
508 recombinant herpes simplex virus 1 lacking both S-component origins of DNA synthesis. J
509 Virol 67:2123–2132.

510 45. Norberg P, Olofsson S, Tarp MA, Clausen H, Bergstrom T, Liljeqvist JA. 2007.
511 Glycoprotein I of herpes simplex virus type 1 contains a unique polymorphic tandem-
512 repeated mucin region. J Gen Virol 88:1683–1688.

513 46. Reynolds AE, Wills EG, Roller RJ, Ryckman BJ, Baines JD. 2002. Ultrastructural
514 localization of the herpes simplex virus type 1 UL31, UL34, and US3 proteins suggests
515 specific roles in primary envelopment and egress of nucleocapsids. J Virol 76:8939–52.

516 47. Roller RJ, Bjerke SL, Haugo AC, Hanson S. 2010. Analysis of a Charge Cluster Mutation of
517 Herpes Simplex Virus Type 1 UL34 and Its Extragenic Suppressor Suggests a Novel
518 Interaction between pUL34 and pUL31 That Is Necessary for Membrane Curvature around
519 Capsids. J Virol 84:3921–3934.

520 48. Buchman TG, Simpson T, Nosal C, Roizman B. 1980. The Stucture of Herpes Simplex Virus
521 DNA and its Application to Molecular Epidemiology. Ann N Y Acad Sci 354:279–290.

522 49. Rastrojo A, López-Muñoz AD, Alcamí A. 2017. Genome Sequence of Herpes Simplex Virus
523 1 Strain SC16. Genome Announc 5:e01392-16.

524 50. Skoblov MY, Lavrov AV, Bragin AG, Zubtsov DA, Andronova VL, Galegov GA, Skoblov
525 YS. 2017. The genome nucleotide sequence of herpes simplex virus 1 strain L2. Russ J
526 Bioorganic Chem 43:140–142.

527 51. Petro CD, Weinrick B, Khajoueinejad N, Burn C, Sellers R, Jacobs WR, Herold BC. 2016.
528 HSV-2 ΔgD elicits FcγR-effector antibodies that protect against clinical isolates. JCI
529 Insight 1.

530 52. Lee K, Kolb AW, Sverchkov Y, Cuellar JA, Craven M, Brandt CR. 2015. Recombination
531 Analysis of Herpes Simplex Virus 1 Reveals a Bias toward GC Content and the Inverted
532 Repeat Regions. J Virol 89:7214–7223.

533 53. Bondre VP, Sankararaman V, Andhare V, Tupekar M, Sapkal GN. 2016. Genetic
534 characterization of human herpesvirus type 1: Full-length genome sequence of strain
535 obtained from an encephalitis case from India. Indian J Med Res 144:750–760.

536 54. Parsons LR, Tafuri YR, Shreve JT, Bowen CD, Shipley MM, Enquist LW, Szpara ML.
537 2015. Rapid Genome Assembly and Comparison Decode Intrastrain Variation in Human
538 Alphaherpesviruses. mBio 6:e02213-14.

539 55. Norberg P, Tyler S, Severini A, Whitley R, Liljeqvist J-A, Bergstrom T. 2011. A genome-
540 wide comparative evolutionary analysis of herpes simplex virus type 1 and varicella zoster
541 virus. PloS One 6:1–8.

542

543 # Tables

544 **Table 1: The Finnish HSV-1 strains used for genome sequence comparisons.**

Sample	Gender	Code	Age	Lesion or diagnosis	Acyclovir sensitivity, IC50 value (µg/ml)
H1211	female	F-11	21	blister	0.25
H1215	male	M-15	5	blister	0.03
H12113	female	F-13	29	blister	0.11
H12114	female	F-14g	23	genital blister	0.50
H12117	female	F-17	57	blister	0.15
H12118	female	F-18g	19	genital blister	0.13
H1311	female	F-11*l*	59	blister (lip)	0.31
H1312	male	M-12	39	blister	0.13
H1412	female	F-12g	28	genital lesion	0.09
H15119	male	M-19	36	blister	0.15

545 *The IC50 value for HSV-1 delta305 (a TK-negative, ACV-resistant, positive-control) was 8.08
546 and for the reference strain HSV-1(17+) it was 0.13. The limit of resistance was ≥2.0 µg/ml.

547

548 **Table 2. Sequencing statistics for Finnish HSV-1 strains.**

Sample	Code	% Depth ≥100	Average coverage	Raw Sequence Reads	Used for Assembly	% Viral	GenBank Accession
H1211	F-11	96%	1,027x	4.2 million	2.8 million	66%	In process^
H1215	M-15	99%	2,808x	5.5 million	3.8 million	70%	In process^
H12113	F-13	98%	2,354x	3.8 million	2.4 million	64%	In process^
H12114	F-14g	98%	2,078x	5.9 million	3.8 million	66%	In process^
H12117	F-17	98%	1,976x	4.1 million	2.7 million	66%	In process^
H12118	F-18g	98%	1,678x	4.2 million	2.9 million	69%	In process^
H1311	F-11*l*	99%	2,541x	4.6 million	3.0 million	65%	In process^
H1312	M-12	98%	2,415x	6.0 million	3.7 million	61%	In process^
H1412	F-12g	98%	1,524x	4.5 million	3.1 million	69%	In process^
H15119	M-19	99%	1,536x	4.8 million	3.0 million	64%	In process^

549 ^See GenBank flatfile attached for review purposes.

550

551 # Figures & Figure Legends

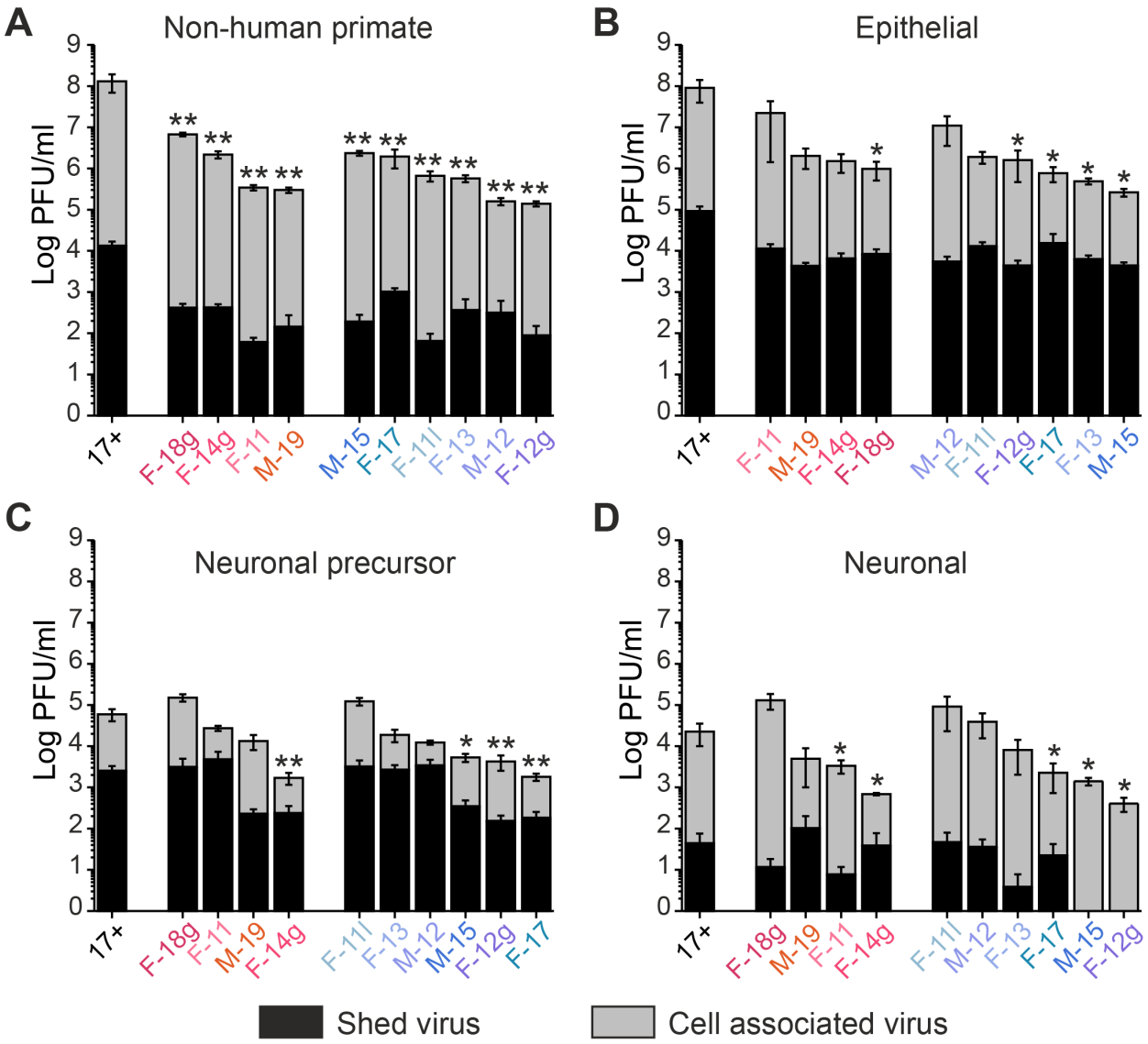

552

553 **Figure 1: Comparison of growth properties of Finnish HSV-1 strains reveals the**

554 **uncoupling of phenotypic and geographic variation.**

555 Histograms comparing virus production for ten Finnish strains of HSV-1, as compared to the

556 HSV-1 reference strain 17+, in different cell types. Panel **(A,** non-human primate**)** shows Vero

557 monkey kidney cells, which are defective in interferon signaling; **(B)** shows HaCaT human
558 epithelial cells; **(C)** shows undifferentiated human SH-SY5Y neuroblastoma cells (neuronal
559 precursor cells); **(D)** shows differentiated human SH-SY5Y neuronal-like cells. Viruses are
560 plotted in descending order based on their viral production, and divided into their genomic sub-
561 groups (see **Figure 4**). Each histogram bar plots infectious virions in the cell-associated fraction
562 (gray) vs. those released from cells (black). **Supplemental Figure S1** shows the same data, but
563 with extracellular released virus plotted as a percentage of total virus production. Bar shows
564 SEM; * = p=<0.05, ** = p<0.001 as compared to the total virus amount (cell associated + shed),
565 clinical isolate vs HSV-1(17+) reference strain.

566

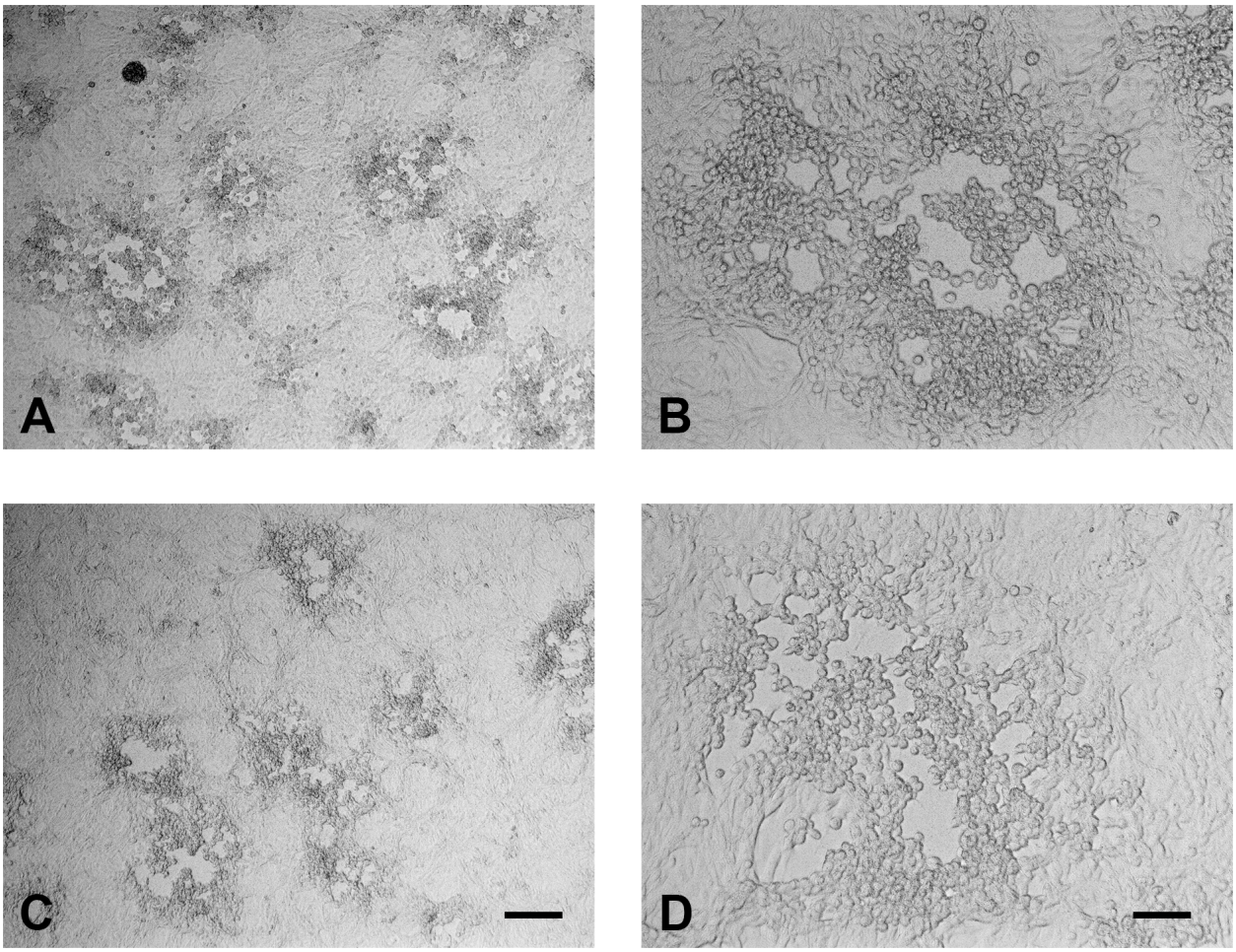

Figure 2. Finnish HSV-1 strains have similar plaque morphology.

Typical morphology of the plaques of the clinical HSV-1 isolates on Vero cells, at 48 hours post infection. Plaques are shown at low magnification (4X, **A,C**), as well as high magnification (10X, **B,D**). Isolates M-19 (**A-B**) and F-12g (**C,D**) serve as representative examples. These two isolates also represent the two sub-groups of Finnish HSV-1 isolates detected in **Figures 3-4**, as well as samples annotated as blister-derived (M-19) and genital-blister-derived (F-12g) (see also **Table 1**). The scale bar corresponds to 100 μm in panels A and C, and to 50 μm in panels B and D.

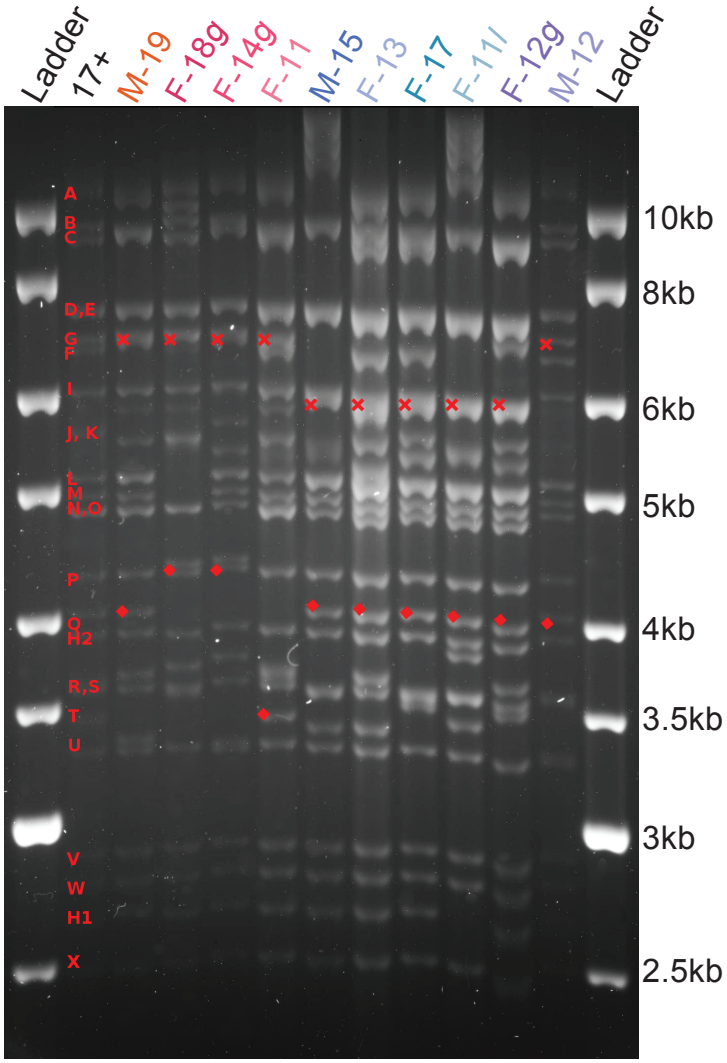

576

577 **Figure 3: RFLP comparison reveals at least two sub-groups of Finnish HSV-1**

578 **strains.**

579 Viral genomic DNA was digested with SalI and separated via electrophoresis to distinguish

580 overall genetic patterns. Classically defined SalI fragment notations (red alphabet letters) are

581 indicated on the left (48). Predicted SalI cut-sites in each viral genome are shown in

582 **Supplemental Figure S2**. Red crosses (x) indicate variation in the size of SalI fragment G, while

583 diamonds indicate variation in the SalI Q fragment.

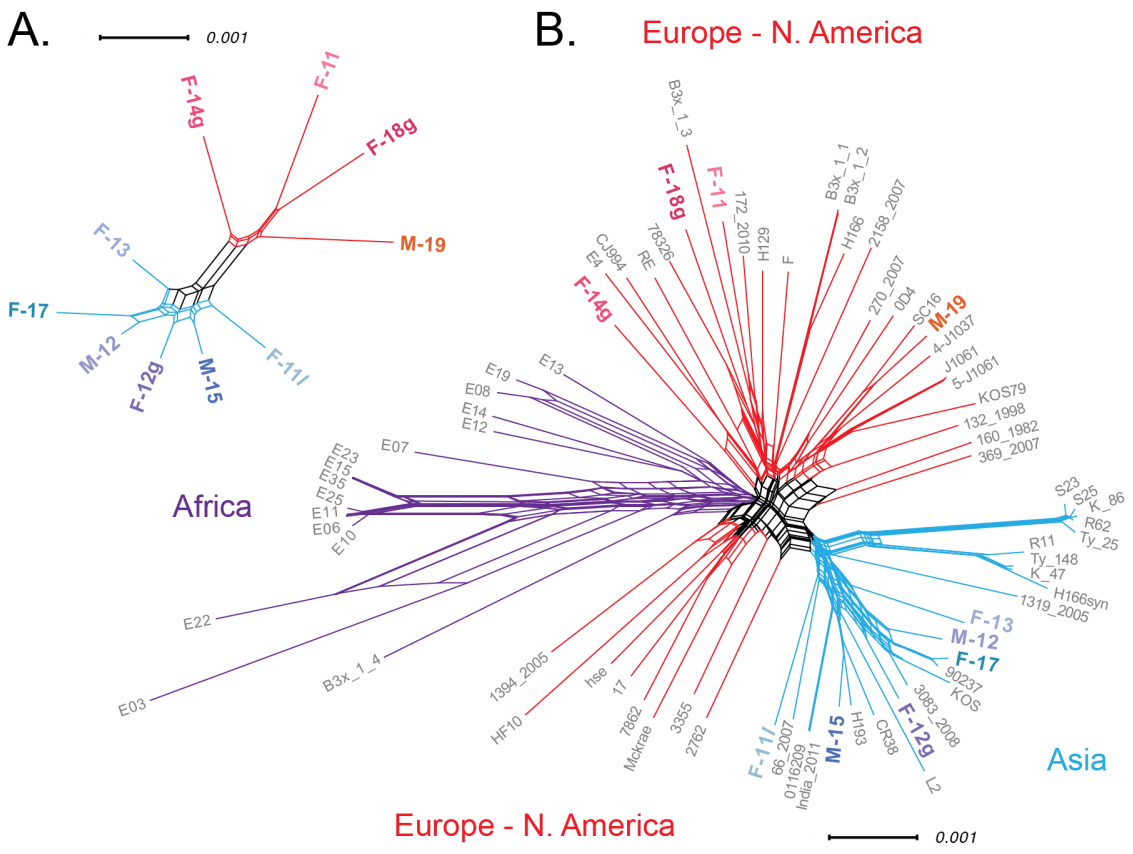

584

585 **Figure 4. A network graph of genetic relatedness reveals that Finland HSV-1**

586 **isolates separate into two sub-groups.**

587 A network graph of genetic relatedness was constructed using SplitsTree4 to demonstrate how

588 the ten new Finland HSV-1 isolates relate to each other (**A**) and to previously described HSV-1

589 genomes from a diversity of locations (**B**). Geographic clustering of branches and clades

590 resemble those previously described (9, 16–18) and are colored by origin of strains: red for

591 Europe and North America, blue for Asia, and purple for Africa. Finland HSV-1 genomes are

592 indicated in bold, and separate into two sub-groups (**A**), which appear to relate previously

593 recognized Asian and European and North American clades. The isolate name, country of origin,

594 GenBank accession, and reference(s) for each previously described HSV-1 genome are listed in

595 **Supplemental Table S1**.

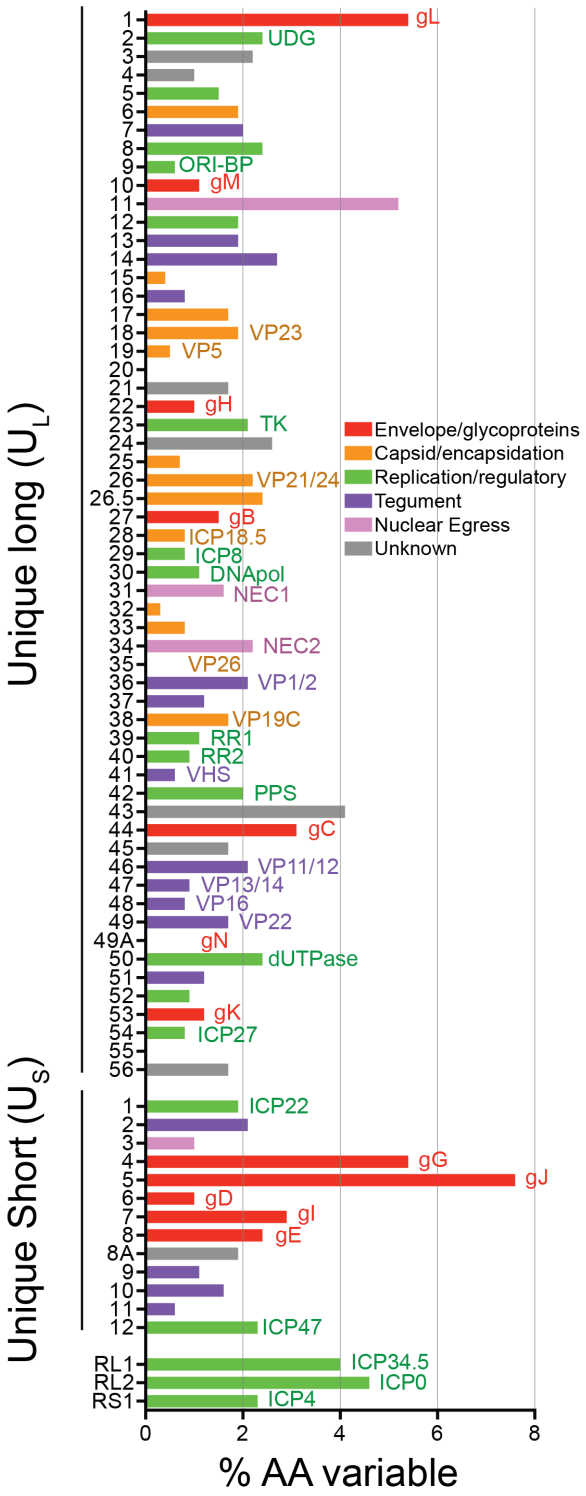

596

597 **Figure 5. Substantial protein-coding variation exists between Finland HSV-1**

598 **isolates.**

599 Histogram showing each protein of the HSV-1 genome and its percent amino acid (AA) variation
600 between the ten Finnish HSV-1 strains compared here. Labels for the Unique Long (UL) and
601 Unique Short (US) regions of the HSV-1 genome are shown in summary format, to the left of
602 each sequentially-numbered viral coding region. Where possible, the common name of each
603 protein is shown to the right of the appropriate histogram bar, e.g. UL1 is also known as gL. AA
604 differences were quantified at the consensus level of each viral genome. See **Supplemental**
605 **Table S2** for additional data on the number of nucleotide differences and dN/dS ratio for each
606 gene.

607

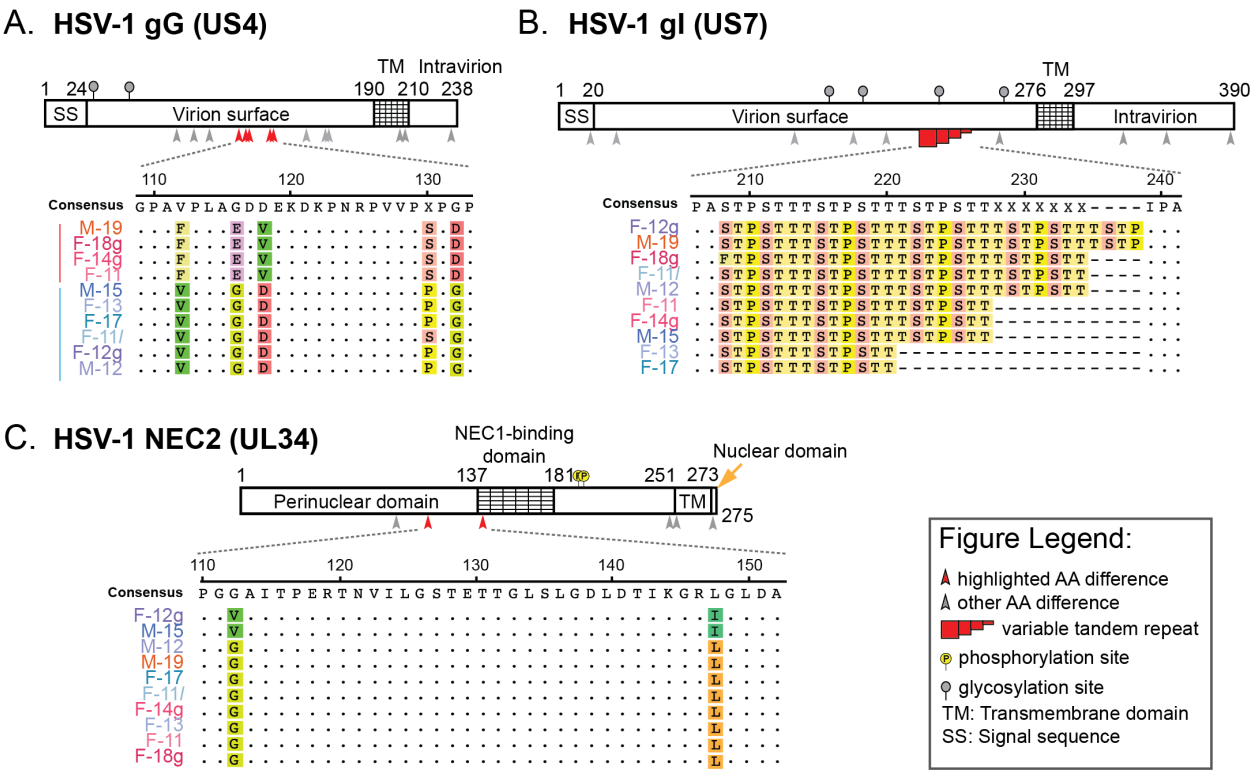

Figure 6. Patterns of genetic variation in Finnish HSV-1 strains correlate with genomic and phenotypic data.

Diagrams depict three HSV-1 proteins with known functional domains and post-translational modifications (e.g. phosphorylation, glycosylation; see Legend). A subset of each protein is highlighted via an AA alignment of the ten clinical HSV-1 isolates. (**A**) Coding differences in the secreted and virion surface glycoprotein G (gG; US4) correlate with the overall genomic sub-groups (clades) shown in **Figure 4**. (**B**) Variation in copy number of a tandem repeat in glycoprotein I (gI; US7) leads to expansion of a repeating tract of mucin-type O-linked glycosylation sites, as described previously in clinical isolates of HSV-1 (16, 45). (**C**) AA differences in the nuclear egress protein NEC2 (UL34) were observed in the two strains (M-15, F-12g) which showed no detectable extracellular virion release in differentiated neuronal cells (**Figure 1D**).

622 # Supplementary Table & Figures

623 **Supplemental Table S1: List of previously published HSV-1 genomes used for**

624 **phylogenetic analyses**

Virus Isolate	Country (with location detail, if available)	GenBank Accession #	References
H1215 / M-15*	Finland	In process	(30), present
H12113 / F-13*	Finland	In process	present
H12117 / F-17*	Finland	In process	(30), present
H1311 / F11*l**	Finland	In process	present
H1312 / M-12*	Finland	In process	present
H1412 / F-12g*	Finland	In process	present
H1211 / F-11*	Finland	In process	(30), present
H12114 / F-14g*	Finland	In process	(30), present
H12118 / F-18g*	Finland	In process	(30), present
H15119 / M-19*	Finland	In process	present
SC16	Spain (Madrid)	KX946970	(49)
172/2010	Germany	LT594105	(12)
2158/2007	Germany	LT594106	(12)
3083/2008	Germany	LT594107	(12)
1319/2005	Germany	LT594108	(12)
270/2007	Germany	LT594109	(12)
66/2007	Germany	LT594110	(12)
1394/2005	Germany	LT594111	(12)
369/2007	Germany	LT594112	(12)
160/1982	Germany	LT594192	(12)
132/1998	Germany	LT594457	(12)
L2	Russia (Moscow)	KT780616	(50)
B^3x1.1	U.S.A. (Bronx, NY)	KU310657	(51)
B^3x1.2	U.S.A. (Bronx, NY)	KU310658	(51)
B^3x1.3	U.S.A. (Bronx, NY)	KU310659	(51)
B^3x1.4	U.S.A. (Bronx, NY)	KU310660	(51)
B^3x1.5	U.S.A. (Bronx, NY)	KU310661	(51)
H193	U.S.A.	KT425108	n/a
KOS79	U.S.A. (Madison, WI)	KT425109	(11)
CJ994	U.S.A. (Madison, WI)	KR011283	(52)
HSV-1/0116209/India/2011	India	KJ847330	(53)
H166	U.S.A.	KM222726	(54)
H166syn	U.S.A.	KM222727	(54)
RE	U.S.A.	KF498959	n/a
OD4	U.S.A. (Madison, WI)	JN420342	(8)
17	U.K. (Glasgow)	JN555585	(9)
CR38	China (Shenyang)	HM585508	(9)

Virus Isolate	Country (with location detail, if available)	GenBank Accession #	References
E03	Kenya (Nairobi)	HM585509	(9)
E06	Kenya (Nairobi)	HM585496	(9)
E07	Kenya (Nairobi)	HM585497	(9)
E08	Kenya (Nairobi)	HM585498	(9)
E10	Kenya (Nairobi)	HM585499	(9)
E11	Kenya (Nairobi)	HM585500	(9)
E12	Kenya (Nairobi)	HM585501	(9)
E13	Kenya (Nairobi)	HM585502	(9)
E14	Kenya (Nairobi)	HM585510	(9)
E15	Kenya (Nairobi)	HM585503	(9)
E19	Kenya (Nairobi)	HM585511	(9)
E22	Kenya (Nairobi)	HM585504	(9)
E23	Kenya (Nairobi)	HM585505	(9)
E25	Kenya (Nairobi)	HM585506	(9)
E35	Kenya (Nairobi)	HM585507	(9)
R11	South Korea (Seoul)	HM585514	(9)
R62	South Korea (Seoul)	HM585515	(9)
S23	Japan (Sapporo)	HM585512	(9)
S25	Japan (Sapporo)	HM585513	(9)
F	U.S.A. (Chicago, IL)	GU734771	(9)
H129	U.S.A. (San Francisco, CA)	GU734772	(9)
McKrae	U.S.A. (Gainesville, FL)	JQ730035, JX142173	(9)
KOS	U.S.A. (Houston, TX)	JQ673480, JQ780693	(9)
HF10	U.S.A. (New York, NY)	DQ889502	(9)
Ty_25	Japan	In process	n/a
Ty_148	Japan	In process	n/a
K_86	Japan	In process	n/a
K_47	Japan	In process	n/a
7-hse †	Sweden or U.S.A.	SRX056767	(55)
7862 †	Sweden or U.S.A.	SRX056770	(55)
3355 †	Sweden or U.S.A.	SRX056769	(55)
2762 †	Sweden or U.S.A.	SRX056768	(55)
90237 †	Sweden or U.S.A.	SRX056772	(55)
E4 †	Sweden or U.S.A.	SRX056773	(55)
78326 †	Sweden or U.S.A.	SRX056771	(55)
4-J1037 †	Sweden or U.S.A.	SRX056760	(55)
J1061 †	Sweden or U.S.A.	SRX056774	(55)
5-J1061	Sweden or U.S.A.	n/a	(55)

625 * newly sequenced strains from Finland in this study.

626 † Sequence data deposited in GenBank short read archive

627

628 **Supplemental Table S2: Number of nucleotide and amino acid (AA) differences observed in each set of Finnish or**

629 **worldwide published HSV1 genomes.**

Gene*	ORF length in NT^	protein length (#AA)	10 Finnish # NT diff.^	10 Finnish # AA changes	10 Finnish %AA diff.	10 Finnish dN/dS	All HSV1 # NT diff.	All HSV1 # AA changes	All HSV1 %AA diff.	All HSV1 dN/dS ratio
UL1	675	224	22	12	5.4	1.20	58	31	13.8	1.15
UL2	1005	334	24	8	2.4	0.50	62	28	8.4	0.82
UL3	675	224	13	5	2.2	0.63	43	19	8.5	0.79
UL4	600	199	11	2	1.0	0.22	43	18	9.0	0.72
UL5	2649	882	35	13	1.5	0.59	106	38	4.3	0.56
UL6	2031	676	43	13	1.9	0.43	107	30	4.4	0.39
UL7	891	296	24	6	2.0	0.33	47	17	5.7	0.57
UL8	2253	750	44	18	2.4	0.69	124	62	8.3	1.00
UL9	2556	851	21	5	0.6	0.31	110	32	3.8	0.41
UL10	1422	473	25	5	1.1	0.25	81	30	6.3	0.59
UL11	291	96	13	5	5.2	0.63	26	17	17.7	1.89
UL12	1881	626	36	12	1.9	0.50	87	30	4.8	0.53
UL13	1557	518	27	10	1.9	0.59	72	33	6.4	0.85
UL14	660	219	10	6	2.7	1.50	27	15	6.8	1.25
UL15	2208	735	22	3	0.4	0.16	80	16	2.2	0.25
UL16	1122	373	13	3	0.8	0.30	55	19	5.1	0.53
UL17	2112	703	30	12	1.7	0.67	108	39	5.5	0.57
UL18	957	318	12	6	1.9	1.00	41	15	4.7	0.58
UL19	4125	1374	39	7	0.5	0.22	139	40	2.9	0.40
UL20	669	222	7	0	0.0	0.00	29	9	4.1	0.45
UL21	1608	535	20	9	1.7	0.82	70	25	4.7	0.56
UL22	2517	838	21	8	1.0	0.62	120	50	6.0	0.71
UL23	1131	376	21	8	2.1	0.62	63	26	6.9	0.70
UL24	810	269	18	7	2.6	0.64	60	28	10.4	0.88

Gene*	ORF length in NT^	protein length (#AA)	10 Finnish # NT diff.^	10 Finnish # AA changes	10 Finnish %AA diff.	10 Finnish dN/dS	All HSV1 # NT diff.	All HSV1 # AA changes	All HSV1 %AA diff.	All HSV1 dN/dS ratio
UL25	1743	580	19	4	0.7	0.27	74	25	4.3	0.51
UL26	1908	635	40	14	2.2	0.54	92	34	5.4	0.59
UL26.5	990	329	21	8	2.4	0.62	45	17	5.2	0.61
UL27	2715	904	51	14	1.5	0.38	123	40	4.4	0.48
UL28	2358	785	26	6	0.8	0.30	87	23	2.9	0.36
UL29	3591	1196	54	10	0.8	0.23	154	33	2.8	0.27
UL30	3708	1235	32	13	1.1	0.68	154	49	4.0	0.47
UL31	921	306	15	5	1.6	0.50	34	13	4.2	0.62
UL32	1791	596	20	2	0.3	0.11	85	28	4.7	0.49
UL33	393	130	2	1	0.8	1.00	14	4	3.1	0.40
UL34	828	275	15	6	2.2	0.67	37	14	5.1	0.61
UL35	339	112	1	0	0.0	0.00	8	1	0.9	0.14
UL36	9420	3139	166	66	2.1	0.66	1271	440	14.0	0.53
UL37	3372	1123	41	13	1.2	0.46	140	60	5.3	0.75
UL38	1398	465	18	8	1.7	0.80	70	30	6.5	0.75
UL39	3414	1137	42	13	1.1	0.45	157	61	5.4	0.64
UL40	1023	340	10	3	0.9	0.43	38	12	3.5	0.46
UL41	1470	489	16	3	0.6	0.23	52	22	4.5	0.73
UL42	1467	488	19	10	2.0	1.11	76	39	8.0	1.05
UL43	1254	417	35	17	4.1	0.94	90	50	12.0	1.25
UL44	1536	511	26	16	3.1	1.60	97	55	10.8	1.31
UL45	519	172	4	3	1.7	3.00	22	8	4.7	0.57
UL46	2157	718	33	15	2.1	0.83	111	65	9.1	1.41
UL47	2082	693	29	6	0.9	0.26	81	29	4.2	0.56
UL48	1473	490	18	4	0.8	0.29	69	25	5.1	0.57
UL49	276	301	13	5	1.7	0.63	42	18	6.0	0.75
UL49A	906	91	2	0	0.0	0.00	8	3	3.3	0.60
UL50	1116	371	23	9	2.4	0.64	65	26	7.0	0.67

Gene*	ORF length in NT^	protein length (#AA)	10 Finnish # NT diff.^	10 Finnish # AA changes	10 Finnish %AA diff.	10 Finnish dN/dS	All HSV1 # NT diff.	All HSV1 # AA changes	All HSV1 %AA diff.	All HSV1 dN/dS ratio
UL51	735	244	12	3	1.2	0.33	33	13	5.3	0.65
UL52	3177	1058	43	9	0.9	0.26	129	41	3.9	0.47
UL53	1017	338	16	4	1.2	0.33	36	12	3.6	0.50
UL54	1539	512	11	4	0.8	0.57	73	34	6.6	0.87
UL55	561	186	5	0	0.0	0.00	25	9	4.8	0.56
UL56	705	234	8	4	1.7	1.00	34	19	8.1	1.27
US10	939	312	11	5	1.6	0.83	65	29	9.3	0.81
US11	486	161	1	1	0.6	1.00	42	19	11.8	0.83
US12	267	88	4	2	2.3	1.00	133	10	11.4	0.08
US1	1263	420	22	8	1.9	0.57	75	39	9.3	1.08
US2	876	291	24	6	2.1	0.33	44	14	4.8	0.47
US3	1446	481	14	5	1.0	0.56	57	21	4.4	0.58
US4	717	238	26	13	5.5	1.00	68	36	15.1	1.13
US5	279	92	10	7	7.6	2.33	25	17	18.5	2.13
US6	1185	394	18	4	1.0	0.29	67	18	4.6	0.37
US7	1173	390	28	12	3.1	0.75	119	57	14.6	0.92
US8	1653	159	30	13	8.2	0.76	302	38	23.9	0.14
US8A	480	550	3	3	0.5	1.00	49	15	2.7	0.44
US9	273	90	1	1	1.1	1.00	12	4	4.4	0.50
RL1	747	248	25	11	4.4	0.79	422	90	36.3	0.27
RL2	2328	775	43	36	4.6	5.14	354	144	18.6	0.69
RS1	3897	1298	62	30	2.3	0.94	345	207	15.9	1.50

630 * See **Supplemental Table S1** for list of strain names and genome accessions for comparisons of 10 Finnish and all published HSV1 genomes.
631 See **Supplemental Table S3** for list of strains excluded from selected gene alignments due to missing data in GenBank.
632 ^ Abbreviations: ORF, open reading frame; NT, nucleotide; AA, amino acid; diff., difference; %, percent; dN/dS, ratio of nonsynonymous to
633 synonymous nucleotide changes

634 **Supplemental Table S3: HSV-1 strains used to calculate nucleotide and amino acid**

635 **(AA) differences in Figure 5 and Supplemental Table S2.**

Gene	# of strains in nucleotide alignment	# of strains in AA alignment	Strains not used in nucleotide and AA alignments*
UL7	60	60	B^3x1.1, B^3x1.2, B^3x1.3, B^3x1.4, B^3x1.5
UL12	61	61	B^3x1.3, B^3x1.4, B^3x1.5, KF498959
UL13	58	58	E06, E25, E11, OD4, B^3x1.3, B^3x1.4, B^3x1.5
UL15	60	60	B^3x1.1, B^3x1.2, B^3x1.3, B^3x1.4, B^3x1.5
UL19	61	61	B^3x1.3, B^3x1.4, B^3x1.5, KF498959
UL26.5	61	61	B^3x1.3, B^3x1.4, B^3x1.5, DQ889502
UL41	61	61	B^3x1.3, B^3x1.4, B^3x1.5, JN420342
UL43	61	61	B^3x1.3, B^3x1.4, B^3x1.5, HF10
UL48	60	60	B^3x1.1, B^3x1.2, B^3x1.3, B^3x1.4, B^3x1.5
UL49A	51	51	B^3x1.3, B^3x1.4, B^3x1.5, DQ889502, LT594110, LT594112, LT594192, LT594111, LT594457, LT594107, LT594106, LT594105, LT594109, LT594108
UL55	59	59	E35, E13, KUTy25, B^3x1.3, B^3x1.4, B^3x1.5
UL56	60	60	B^3x1.3, B^3x1.4, B^3x1.5, HM585507, DQ889502
US1	60	60	B^3x1.1, B^3x1.2, B^3x1.3, B^3x1.4, B^3x1.5
US8A	61	61	HF10, B^3x1.3, B^3x1.4, B^3x1.5
RL1	58	58	B^3x1.3, B^3x1.4, B^3x1.5, JN420342, LT594111, KR011283, KT780616
RL2	61	61	B^3x1.3, B^3x1.4, B^3x1.5, B^3x1.2
RS1	59	59	B^3x1.3, B^3x1.4, B^3x1.5, HM585512, KR011283, KT780616
All other genes	62	62	B^3x1.3, B^3x1.4, B^3x1.5

636 * Strains were excluded due to missing data (e.g. due to sequencing gaps) or annotations in
637 GenBank.
638

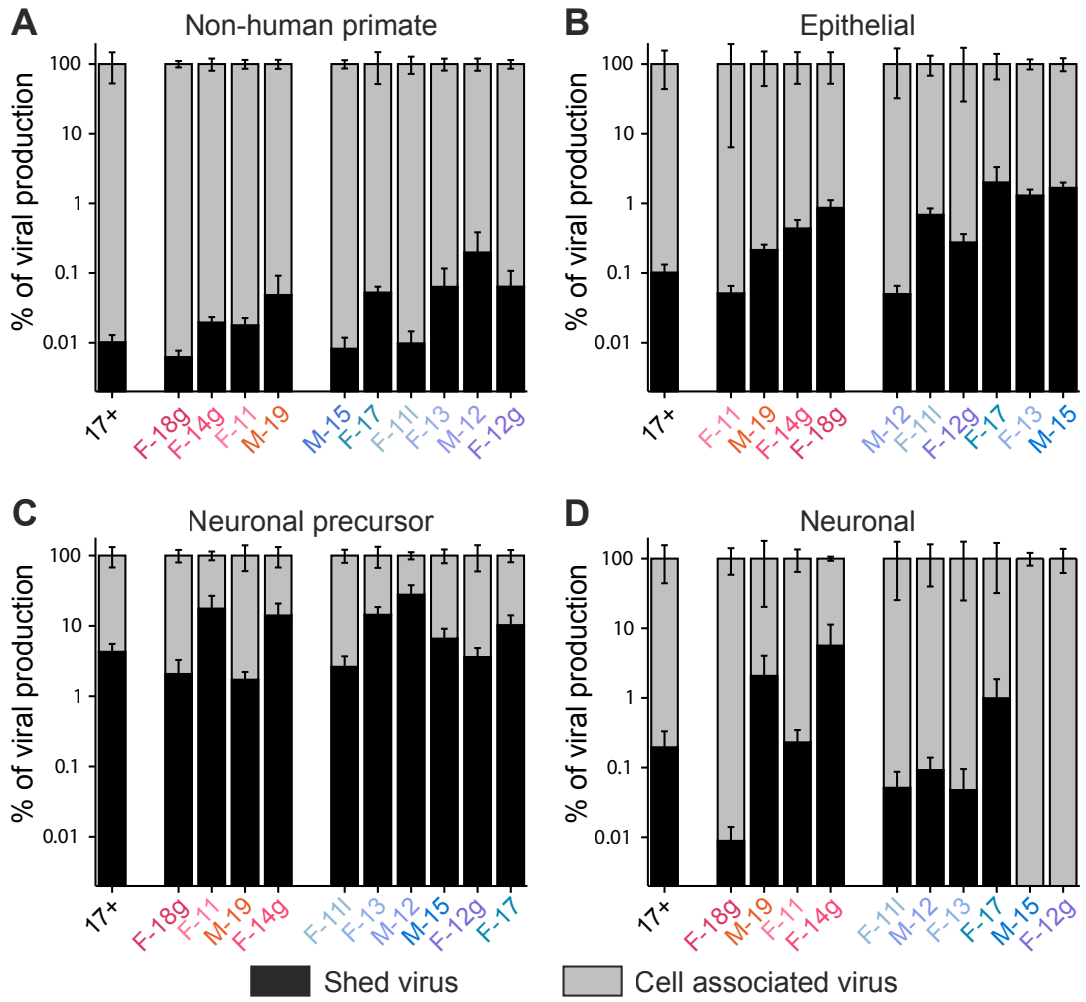

Supplemental Figure S1. Viral production as percent values in shed and cell-associated fractions.

Histograms compare virus production for ten Finnish strains of HSV-1, as compared to the HSV-1 reference strain 17+, in different cell types. These data are the same as those shown in **Figure 1**, but here extracellular released virus, or shed virus (black), is plotted as a percentage of total virus production (gray). Viruses are plotted in the same order as **Figure 1**, which is descending based on their viral production, within each genomic sub-group (see **Figure 4**). Panel (**A,** non-human primate) shows Vero monkey kidney cells, which are defective in interferon signaling;

648 **(B)** shows HaCaT human epithelial cells; **(C)** shows undifferentiated human SH-SY5Y
649 neuroblastoma cells (neuronal precursor cells); **(D)** shows differentiated human SH-SY5Y
650 neuronal-like cells. Bar shows SEM.

651

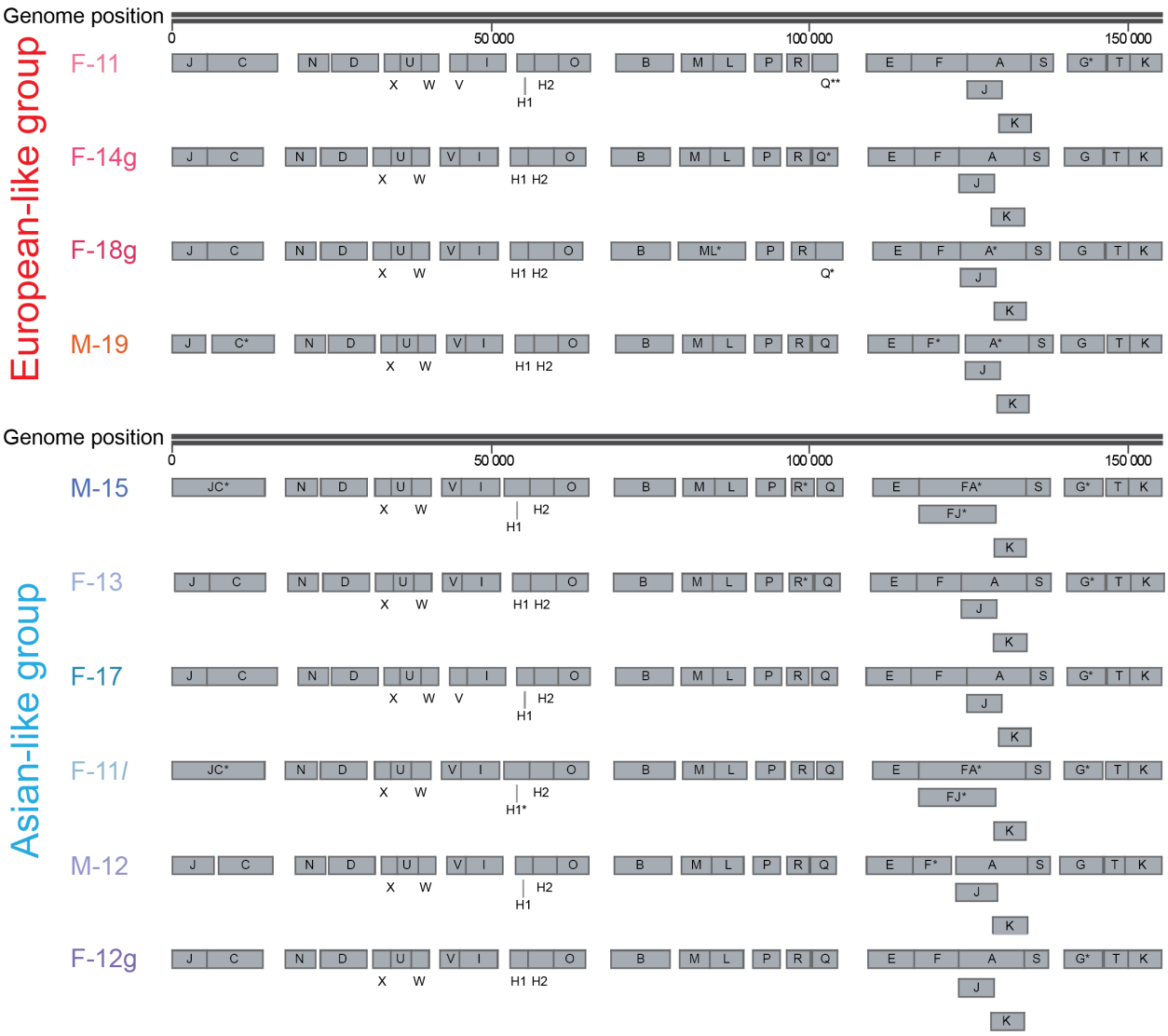

Supplemental Figure S2: Diagrams depict the predicted SalI cut-sites in 10 Finnish HSV-1 genomes.

A computational prediction of SalI restriction sites is shown for each viral consensus genome. Classically defined SalI fragment notations (alphabet letters) are indicated on each major fragment. These maps were compared to the experimentally observed fragments in **Figure 3**. Genomic sub-groups are as diagrammed in **Figure 4**.

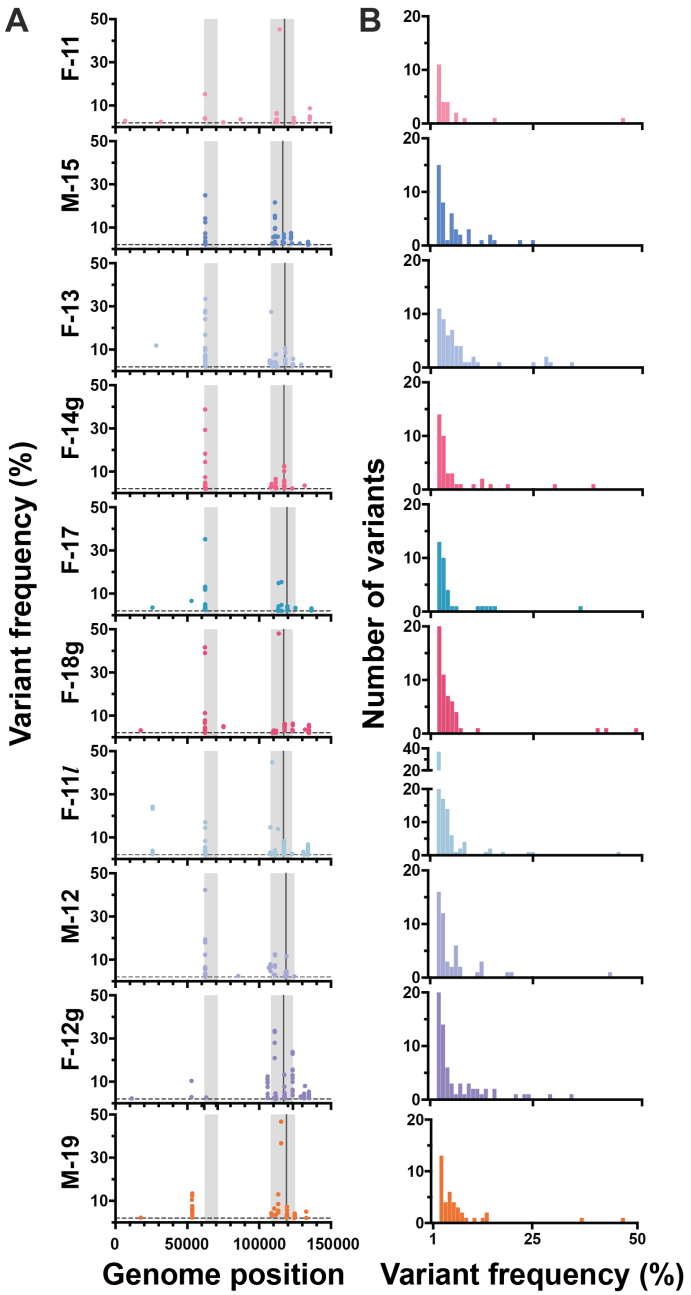

659

660 **Supplemental Figure S3. Scatter plots demonstrate the distribution of minority**

661 **variants in each Finnish HSV-1 genome.**

662 **(A)** Scatter plots demonstrate the position (x-axis) and frequency (y-axis) of minority variants

663 detected in each Finnish HSV-1 genome. The limit of detection was set at 2% (see Methods for

664 details). Stochastic aspects of alignment at tandem repeats can generate excess signals of

665 minority variants near these areas, as can be seen in VP1/2 (UL36) and in the internal-repeat
666 regions (areas denoted in gray on x-axis). **(B)** Histograms depict the total number of minority
667 variants (y-axis) in each frequency bin (x-axis) for each strain of Finnish HSV-1. Bins are in 1%
668 increments.

669